MEDS Clinical Medicine (2026)
Clausius Scientific Press, Canada

DOI: 10.23977/medsc.2026.070402
ISSN 2616-1907 Vol. 7 Num. 4

Therapeutic Mechanism of Siraitia grosvenorii Against MAFLD: Integrated Multi-Omics and Genetic Causal Analysis

Baoshan Tang[1,a,#], Guihong Liu[1,b,#] , Yijia Li[1,c], Hui Tang[1,d,*]

[1]Guangxi Key Laboratory of Molecular Medicine in Liver Injury and Repair, the First Affiliated Hospital of Guilin Medical University, Guilin, 541001, Guangxi, China
[a]284859952@qq.com, [b]2270539909@qq.com, [c]3492796448@qq.com, [d]jonobel@163.com
[#]Baoshan Tang and Guihong Liu contributed equally to this work.
**Corresponding author*

Keywords: MAFLD, Siraitia grosvenorii; Mendelian randomization; PIK3CG; Single-cell RNA sequencing; Molecular dynamics

Abstract: Metabolic-associated fatty liver disease (MAFLD) currently lacks targeted pharmacotherapies. This study explored the multi-target mechanisms underlying the protective action of Siraitia grosvenorii against MAFLD by integrating multi-omics analyses and a genetic causal inference framework. Network pharmacology was used to screen bioactive compounds and disease-related targets, while weighted gene co-expression network analysis (WGCNA) of transcriptomic datasets GSE174478 and GSE193066 was performed to identify hub genes associated with clinical phenotypes. Two-sample Mendelian randomization (MR) was adopted to assess the genetically causal relationships with MAFLD, alanine transaminase (ALT) and aspartate transaminase (AST). Single-cell RNA sequencing data (GSE174748) was applied to characterize the cellular localization of target gene expression, and molecular docking combined with 10 ns molecular dynamics (MD) simulations was carried out to validate the structural binding stability. We identified 11 bioactive compounds and 54 overlapping disease targets, whose functional enrichment was mainly concentrated in the TNF, NF-κB and PI3K-Akt signaling pathways. MR analysis identified PIK3CG as the core therapeutic target, which exerted a robust causal protective effect on MAFLD (IVW OR = 0.879, P = 0.038), ALT (OR = 0.975, P = 0.004), and AST (OR = 0.973, P = 0.0026). Single-cell profiling revealed that PIK3CG was predominantly expressed in intrahepatic immune cells, including macrophages, T cells and dendritic cells. Molecular docking and MD simulations verified high-affinity binding and favorable conformational stability between PIK3CG and beta-sitosterol (−8.455 kcal/mol), as well as kaempferol (−8.707 kcal/mol), with low RMSD (< 2.5 Å) and RMSF (< 4.0 Å) trajectories. Collectively, S. grosvenorii confers protective effects against MAFLD principally through PIK3CG-dependent immune-metabolic regulation, representing a validated natural product-based therapeutic strategy.

1. Introduction

Metabolic-associated fatty liver disease (MAFLD), encompassing simple steatosis, metabolic steatohepatitis (MASH), and liver cirrhosis, affects over 25% of the global adult population [1, 2]. Driven by lipotoxicity, chronic inflammation, and oxidative stress, MAFLD represents a critical healthcare burden currently lacking approved targeted pharmacotherapies [1, 2]. Siraitia grosvenorii (Swingle), a traditional medicinal herb native to southern China, exhibits diverse pharmacological activities including antioxidant, anti-inflammatory, and metabolic regulatory properties[3] . Recent experimental studies demonstrate that S. grosvenorii extracts attenuate hepatic steatosis and inflammatory injury in dietary animal models[4, 5] .

Network pharmacology and multi-omics frameworks offer powerful approaches to decipher the complex multi-target mechanisms of traditional Chinese medicines[6, 7] . However, conventional observational analyses remain vulnerable to residual confounding and reverse causation. Mendelian randomization (MR) utilizes genetic variants as instrumental variables to infer unconfounded causal relationships between exposures and disease outcomes [8]. In this study, we integrated network pharmacology, transcriptomic Weighted Gene Co-expression Network Analysis (WGCNA), two-sample MR causal inference, single-cell RNA sequencing, and 10 ns molecular dynamics (MD) simulations. This holistic approach isolated PIK3CG as a core therapeutic target and elucidated the multi-pathway mechanism through which S. grosvenorii protects against MAFLD.

2. Materials and Methods

2.1. Screening Active Components and Target Identification

Bioactive constituents of S. grosvenorii were obtained from the Traditional Chinese Medicine Systems Pharmacology Database (TCMSP)[7] . Compounds were filtered using oral bioavailability (OB) ≥ 30% and drug-likeness (DL) ≥ 0.8 thresholds[6, 7] . Associated target proteins were retrieved and standardized to official human gene symbols via UniProt. Disease targets associated with MAFLD were compiled from OMIM, TTD, and GeneCards databases, and intersecting targets between S. grosvenorii and MAFLD were identified using Venn diagram analysis.

2.2. PPI Network and Enrichment Analysis

Protein-protein interaction (PPI) networks were constructed using STRING (v11.5) with a confidence score threshold ≥ 0.4 and visualized in Cytoscape (v3.9.1)[9] . Gene Ontology (GO) and Kyoto Encyclopedia of Genes and Genomes (KEGG) pathway enrichment analyses were conducted using the R package clusterProfiler ($P < 0.05$).

2.3. Transcriptomic WGCNA and Hub Gene Selection

WGCNA was performed on GEO microarray datasets GSE174478 and GSE193066 using the R package WGCNA [10]. Co-expression modules significantly correlated with fibrosis stage and NAFLD activity score (NAS) were identified. Candidate hub genes were determined by intersecting clinical module genes with predicted drug-disease shared targets.

2.4. Two-Sample Mendelian Randomization Causal Inference

Two-sample MR analysis was executed using the TwoSampleMR package[8] . Instrumental variables (IVs) for candidate hub genes were selected at $P < 5\times10^{-6}$, linkage disequilibrium $r^2 < 0.2$,

and a 10,000 kb clumping window. Inverse variance weighted (IVW) served as the primary statistical method, supplemented by MR-Egger, Weighted Median, Simple Mode, and Weighted Mode methods. Sensitivity analyses included MR-Egger intercept tests for horizontal pleiotropy.

2.5. Single-Cell RNA Sequencing and Molecular Dynamics Simulations

Single-cell dataset GSE174748 was processed using Seurat (v4.0)[11]. Quality control retained cells with 200 < nFeature_RNA < 2000 and percent.mt < 20%. Batch effects were corrected via Harmony, followed by cell clustering and annotation. Molecular docking and 10 ns MD simulations were performed in YASARA under the AMBER03 force field [8]. Backbone root-mean-square deviation (RMSD) and root-mean-square fluctuation (RMSF) metrics were quantified over the 10 ns trajectory.

3. Results

3.1. Active Compounds and Common Targets

Screening identified 11 active compounds of S. grosvenorii interacting with 81 target genes. Intersecting these with 3,414 retrieved MAFLD disease targets yielded 54 shared therapeutic targets. Network topology highlighted 6 core active constituents: beta-sitosterol, kaempferol, flazin, mandenol, perlolyrine, and ZINC03860434 (Figures 1).

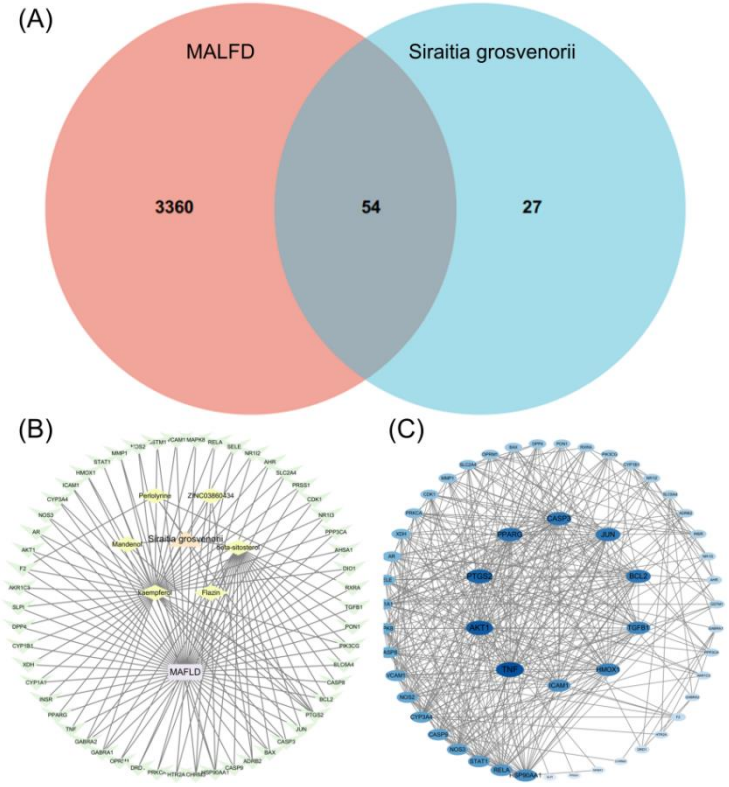

Figure 1. Construction of the "Drug-Disease-Active Components-Targets" Network. (A) Venn diagram showing the common targets between Siraitia grosvenorii and MAFLD. (B) "Drug-Disease-Active Components-Targets" network. (C) Protein-protein interaction network of the common targets.

3.2. Functional and Pathway Enrichment

GO enrichment demonstrated significant involvement in xenobiotic stimulus response, reactive oxygen species regulation, and lipopolysaccharide cellular response. KEGG analysis mapped key enrichments to the TNF, Apoptosis, HIF-1, NF-κB, and PI3K-Akt signaling pathways, highlighting comprehensive anti-inflammatory and metabolic modulation (Figures 2).

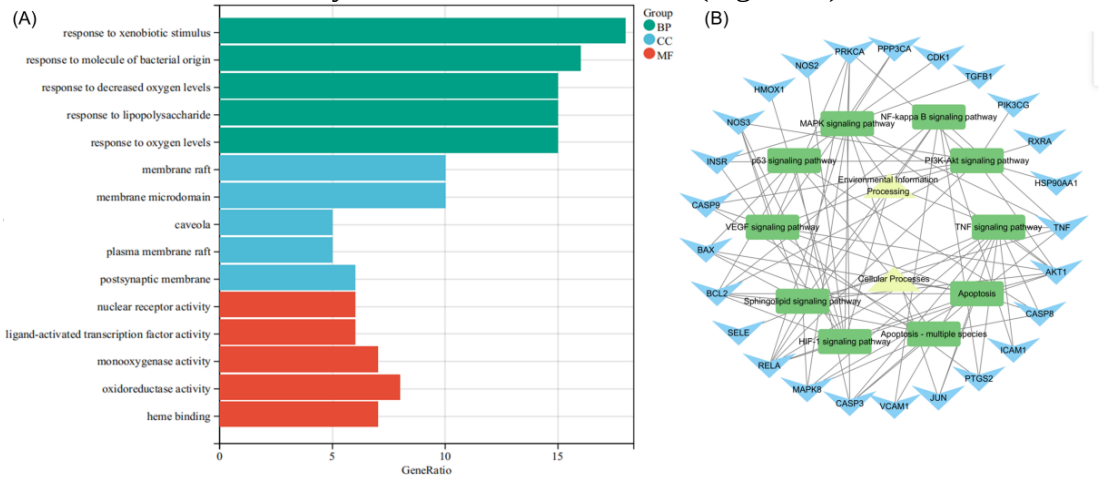

Figure 2. Enrichment Analysis of Common Target Genes. (A) Results of the GO enrichment analysis for common target genes. (B) Results of the KEGG enrichment analysis for common target genes.

3.3. WGCNA and Mendelian Randomization Identification of PIK3CG

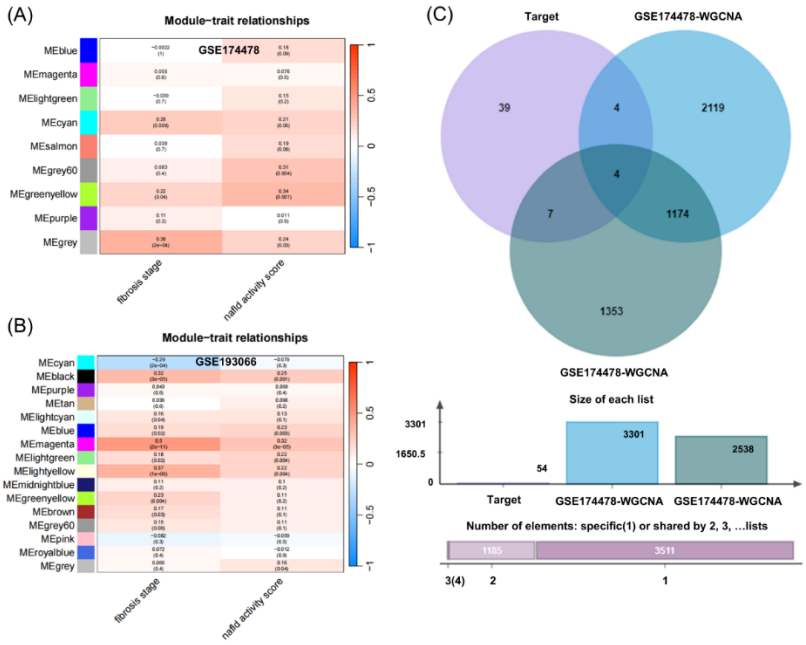

Figure 3. Screening of MAFLD Clinically Relevant Genes. (A) WGCNA module correlation with fibrosis stage and NAFLD activity score in the GSE174478 dataset. (B) WGCNA module correlation with fibrosis stage and NAFLD activity score in the GSE193066 dataset. (C) Venn diagram of intersecting genes from WGCNA analyses and predicted target genes, identifying TGFB1, PIK3CG, NOS3, and CASP8 as the key genes.

WGCNA on GSE174478 and GSE193066 identified trait-associated modules correlated with fibrosis stage and NAS score. Intersecting module genes with shared targets isolated 4 hub candidate genes: TGFB1, PIK3CG, NOS3, and CASP8 (Figures 3). Two-sample MR causal analysis established that PIK3CG conferred statistically significant causal protection against MAFLD risk (IVW OR = 0.879, 95% CI: 0.779–0.992, P = 0.038), ALT elevation (IVW OR = 0.975, 95% CI: 0.958–0.992, P = 0.004), and AST elevation (IVW OR = 0.973, 95% CI: 0.956–0.990, P = 0.00263) (Table 1). CASP8 was causally linked only to ALT (OR = 0.974, P = 9.72×10^{-6}), whereas NOS3 showed no significant causal effect.

Table 1. Two-sample Mendelian Randomization analysis of candidate hub genes across MAFLD and liver injury biomarkers.

Outcome Trait	Exposure Gene	Method	P-value	OR (95% CI)
MAFLD	CASP8	IVW	0.5010	1.020 (0.963–1.081)
MAFLD	NOS3	IVW	0.2360	1.049 (0.969–1.135)
MAFLD	PIK3CG	IVW	0.0380*	0.879 (0.779–0.992)
ALT	CASP8	IVW	9.72e-06***	0.974 (0.963–0.985)
ALT	NOS3	IVW	0.1170	1.010 (0.998–1.022)
ALT	PIK3CG	IVW	0.0040**	0.975 (0.958–0.992)
AST	CASP8	IVW	0.1460	0.992 (0.981–1.003)
AST	NOS3	IVW	0.5100	0.996 (0.984–1.008)
AST	PIK3CG	IVW	0.0026**	0.973 (0.956–0.990)

Abbreviations: IVW, Inverse Variance Weighted; OR, Odds Ratio; ALT, Alanine Aminotransferase; AST, Aspartate Aminotransferase. *P < 0.05, **P < 0.01, ***P < 0.001.

3.4. Single-Cell Profiling

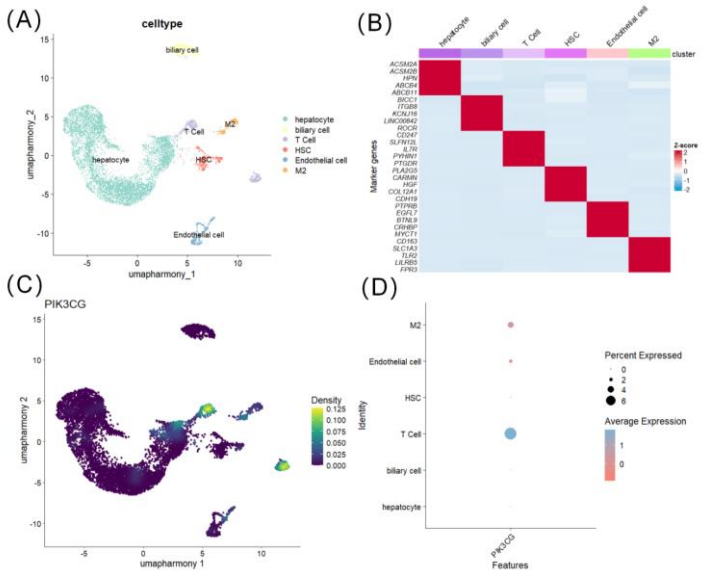

Figure 4: Expression of PIK3CG at the Single-Cell Level. (A) Annotation results of the GSE174748 data, depicting the variety of cell types identified in the single-cell analysis. (B) Expression of top5 marker genes for each cell type, confirming the distinct identities of the cellular populations within the dataset. (C) and (D) : Expression levels of PIK3CG across various cell types, highlighting its specific expression patterns in T cells. These panels illustrate the transcriptional profile of PIK3CG within the immune cell subsets, suggesting its potential immunomodulatory role in MAFLD.

Single-cell RNA sequencing of GSE174748 resolved 14 intrahepatic cell clusters [9]. Cellular localization revealed that PIK3CG expression is predominantly enriched in immune cells, specifically M1 macrophages, CD8+ T cells, and resting dendritic cells (Figures 4).

3.5. Molecular Binding Stability and Trajectory Dynamics

Molecular docking confirmed robust structural affinities between PIK3CG and major S. grosvenorii bioactives, yielding binding energies of -8.455 kcal/mol for beta-sitosterol and -8.707 kcal/mol for kaempferol (Figures 5 AB). Key hydrogen bonding and hydrophobic interactions stabilized the active catalytic pocket. During 10 ns explicit-solvent MD simulations, backbone RMSD values rapidly converged within 2 ns and remained exceedingly stable below 2.5 Å throughout the trajectory (Figures 5C). RMSF analysis demonstrated low root-mean-square fluctuations (< 4.0 Å) across all amino acid residues, confirming structural rigidity and thermodynamic favorability (Figures 5 D).

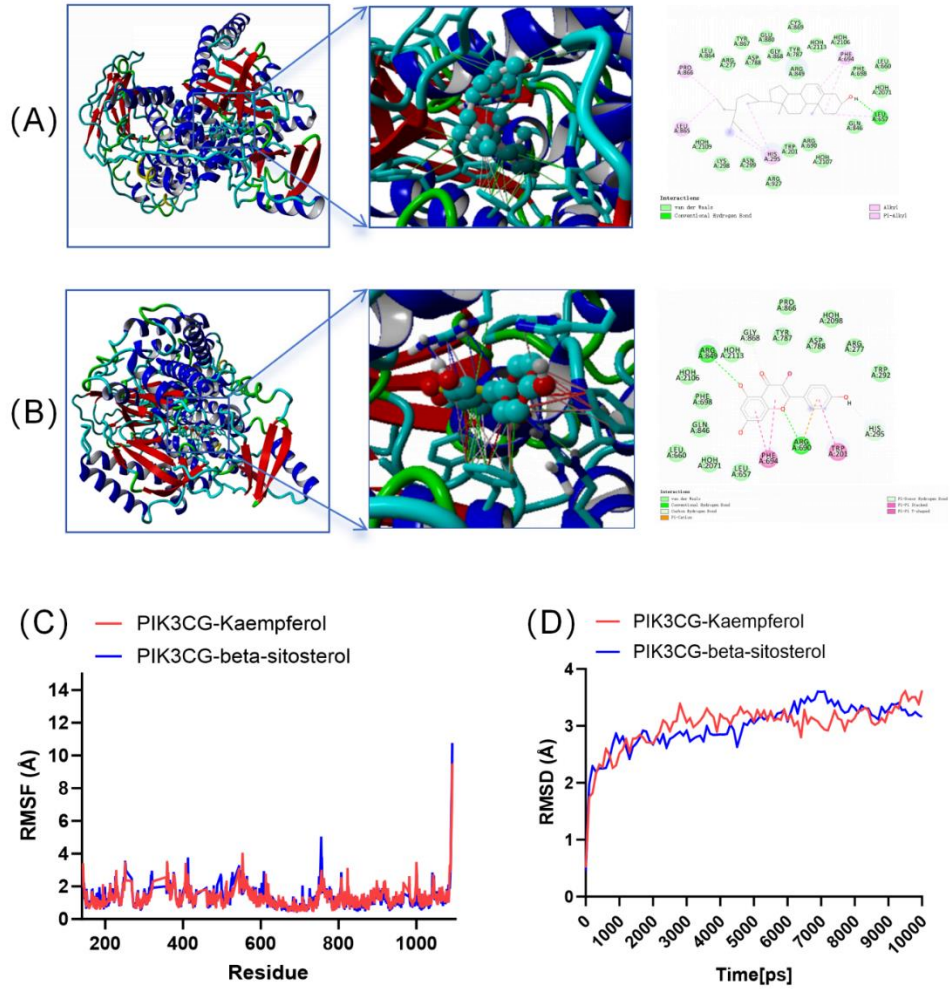

Figure 5: Molecular Docking of Core Gene with Corresponding Compounds. (A) Docking results of PIK3CG with beta-sitosterol, showcasing the interaction between the protein and the compound, including the binding pose and the calculated binding affinity(Vina score -8.455 kcal/mol). (B) Docking results of PIK3CG with Kaempferol, demonstrating the potential binding mode and the estimated strength of the interaction between the protein and the compound(Vina score -8.707 kcal/mol). (C) RMSF of PIK3CG-compound. (D) RMSD of PIK3CG-compound.

4. Discussion

MAFLD progression is driven by a complex interplay between hepatic lipotoxicity, oxidative stress, and chronic low-grade inflammation[1, 12, 13]. Natural Chinese medicinal herbs present multi-target therapeutic potential for complex metabolic diseases [3, 6]. S. grosvenorii extracts have demonstrated hepatoprotective and anti-inflammatory efficacy in animal models [4, 5, 14]. In this study, multi-omics integration and genetic causal inference identified PIK3CG as a crucial protective hub gene in MAFLD.

Pathway enrichment highlighted the involvement of TNF, NF-κB, and PI3K-Akt cascades [15-17]. PIK3CG (encoding PI3Kγ) plays a central role in modulating immune cell trafficking and inflammatory signal transduction[16, 18]. Our single-cell analysis mapped PIK3CG expression primarily to intrahepatic M1 macrophages, T cells, and dendritic cells. In fatty liver pathology, activation of PI3Kγ in Kupffer cells and infiltrating macrophages drives inflammatory cytokine secretion and metabolic dysregulation [16, 18]. Pharmacological or genetic modulation of PI3Kγ attenuates hepatic steatohepatitis and fibrosis[16].

Mendelian randomization provides strong genetic causal evidence that higher genetically predicted PIK3CG expression lowers MAFLD susceptibility and reduces ALT/AST liver injury markers, mitigating observational confounding [8, 19]. Furthermore, molecular docking and MD simulations established that S. grosvenorii key active compounds—beta-sitosterol and kaempferol—bind stably within the PIK3CG catalytic pocket[20]. Beta-sitosterol and kaempferol have been widely reported to reduce hepatic steatosis, alleviate oxidative stress, and suppress inflammatory cytokine release[21-24]. Our findings link these active constituents directly to PIK3CG-mediated immune-metabolic regulation.

Limitations: Although this study combines multi-omics, causal inference, and molecular simulations, experimental in vitro and in vivo studies are necessary to confirm the precise biochemical inhibition or activation dynamics of S. grosvenorii compounds on PIK3CG.

5. Conclusion

In conclusion, this study demonstrates that Siraitia grosvenorii exerts multi-target hepatoprotective effects against MAFLD primarily via PIK3CG-mediated immune-metabolic regulation. Beta-sitosterol and kaempferol represent key active constituents demonstrating high conformational stability with PIK3CG. These findings provide a solid theoretical foundation for S. grosvenorii as a natural pharmacological agent for MAFLD.

Acknowledgements

The public datasets analyzed in this study were obtained from the Gene Expression Omnibus (GSE174478, GSE193066, GSE174748) and the TCMSP database. We appreciate the researchers who contributed data to the GEO repository. The present study was supported by the Guangxi Graduate Innovation Project (No. YCSW2025485) and the College Students' Innovation and Entrepreneurship Training Program of Guilin Medical University(No. 202410601003).

References

[1] Eslam, M., A.J. Sanyal, J. George, and P. International Consensus, (2020) MAFLD: A Consensus-Driven Proposed Nomenclature for Metabolic Associated Fatty Liver Disease. Gastroenterology, 158(7): p. 1999-2014 e1.

[2] Younossi, Z., F. Tacke, M. Arrese, B. Chander Sharma, I. Mostafa, E. Bugianesi, V. Wai-Sun Wong, Y. Yilmaz, J. George, J. Fan, and M.B. Vos, (2019) Global Perspectives on Nonalcoholic Fatty Liver Disease and Nonalcoholic Steatohepatitis. Hepatology, 69(6): p. 2672-2682.

[3] Wu, J., Y. Jian, H. Wang, H. Huang, L. Gong, G. Liu, Y. Yang, and W. Wang, (2022) A Review of the Phytochemistry and Pharmacology of the Fruit of Siraitia grosvenorii (Swingle): A Traditional Chinese Medicinal Food. Molecules, 27(19).
[4] Uno, K., K. Miyajima, S. Ogawa, N. Suzuki-Kemuriyama, and D. Nakae, (2023) Effects of Siraitia grosvenorii extract on nonalcoholic steatohepatitis-like lesions in Sprague Dawley rats fed a choline-deficient, methionine-lowered, l-amino acid-defined diet. J Toxicol Pathol, 36(1): p. 1-10.
[5] Lu, R., J. Hu, X. Liu, L. Yu, J. Hu, H. Jiang, S. Liu, M. Li, J. He, X. Yang, and X. Liang, (2023) Mogroside-rich extract from Siraitia grosvenorii fruits protects against heat stress-induced intestinal damage by ameliorating oxidative stress and inflammation in mice. Food Funct, 14(2): p. 1238-1247.
[6] Zhang, R., X. Zhu, H. Bai, and K. Ning, (2019) Network Pharmacology Databases for Traditional Chinese Medicine: Review and Assessment. Front Pharmacol, 10: p. 123.
[7] Ru, J., P. Li, J. Wang, W. Zhou, B. Li, C. Huang, P. Li, Z. Guo, W. Tao, Y. Yang, X. Xu, Y. Li, Y. Wang, and L. Yang, (2014) TCMSP: a database of systems pharmacology for drug discovery from herbal medicines. J Cheminform, 6: p. 13.
[8] Hemani, G., J. Zheng, B. Elsworth, K.H. Wade, V. Haberland, D. Baird, C. Laurin, S. Burgess, J. Bowden, R. Langdon, V.Y. Tan, J. Yarmolinsky, H.A. Shihab, N.J. Timpson, D.M. Evans, C. Relton, R.M. Martin, G. Davey Smith, T.R. Gaunt, and P.C. Haycock, (2018) The MR-Base platform supports systematic causal inference across the human phenome. Elife, 7.
[9] Szklarczyk, D., A.L. Gable, D. Lyon, A. Junge, S. Wyder, J. Huerta-Cepas, M. Simonovic, N.T. Doncheva, J.H. Morris, P. Bork, L.J. Jensen, and C.V. Mering, (2019) STRING v11: protein-protein association networks with increased coverage, supporting functional discovery in genome-wide experimental datasets. Nucleic Acids Res, 47(D1): p. D607-D613.
[10] Langfelder, P. and S. Horvath, (2008) WGCNA: an R package for weighted correlation network analysis. BMC Bioinformatics, 9: p. 559.
[11] Hao, Y., S. Hao, E. Andersen-Nissen, W.M. Mauck, 3rd, S. Zheng, A. Butler, M.J. Lee, A.J. Wilk, C. Darby, M. Zager, P. Hoffman, M. Stoeckius, E. Papalexi, E.P. Mimitou, J. Jain, A. Srivastava, T. Stuart, L.M. Fleming, B. Yeung, A.J. Rogers, J.M. McElrath, C.A. Blish, R. Gottardo, P. Smibert, and R. Satija, (2021) Integrated analysis of multimodal single-cell data. Cell, 184(13): p. 3573-3587 e29.
[12] Schuster, S., D. Cabrera, M. Arrese, and A.E. Feldstein, (2018) Triggering and resolution of inflammation in NASH. Nat Rev Gastroenterol Hepatol, 15(6): p. 349-364.
[13] Gallage, S., O. Govaere, Q.M. Anstee, G.I. Shulman, F. Tacke, and M. Heikenwalder, (2026) Molecular mechanisms and pathogenesis of MASH. Nature, 657(8130): p. 59-75.
[14] Li, L., W. Zheng, C. Wang, J. Qi, and H. Li, (2020) Mogroside V Protects against Hepatic Steatosis in Mice on a High-Fat Diet and LO2 Cells Treated with Free Fatty Acids via AMPK Activation. Evid Based Complement Alternat Med, p. 7826874.
[15] Li, J., T. Wang, P. Liu, F. Yang, X. Wang, W. Zheng, and W. Sun, (2021) Hesperetin ameliorates hepatic oxidative stress and inflammation via the PI3K/AKT-Nrf2-ARE pathway in oleic acid-induced HepG2 cells and a rat model of high-fat diet-induced NAFLD. Food Funct, 12(9): p. 3898-3918.
[16] Zhang, W., Y. Liu, M. Wu, X. Zhu, T. Wang, K. He, P. Li, and X. Wu, (2017) PI3K inhibition protects mice from NAFLD by down-regulating CMKLR1 and NLRP3 in Kupffer cells. J Physiol Biochem, 73(4): p. 583-594.
[17] Pan, Y., L. Qiao, Y. Zhang, S.R. Sooranna, D. Huang, M. Ou, F. Xu, L. Chen, and D. Huang, (2024) The molecular and network mechanisms of antilipidemic potential effects of Ganfule capsules in nonalcoholic fatty liver disease. Heliyon, 10(14): p. e34297.
[18] Amano, M.T., A. Castoldi, V. Andrade-Oliveira, M.T. Latancia, F.F. Terra, M. Correa-Costa, C.N.S. Breda, R.J.F. Felizardo, W.O. Pereira, M.B. da Silva, M.Y.S. Miyagi, C.F. Aguiar, M.I. Hiyane, J.S. Silva, I.C. Moura, and N.O.S. Camara, (2018) The lack of PI3Kgamma favors M1 macrophage polarization and does not prevent kidney diseases progression. Int Immunopharmacol, 64: p. 151-161.
[19] Zheng, K.I., J.G. Fan, J.P. Shi, V.W. Wong, M. Eslam, J. George, and M.H. Zheng, (2020) From NAFLD to MAFLD: a "redefining" moment for fatty liver disease. Chin Med J (Engl), 133(19): p. 2271-2273.
[20] Krieger, E. and G. Vriend, (2014) YASARA View-molecular graphics for all devices-from smartphones to workstations. Bioinformatics, 30(20): p. 2981-2.
[21] Feng, S., L. Gan, C.S. Yang, A.B. Liu, W. Lu, P. Shao, Z. Dai, P. Sun, and Z. Luo, (2018) Effects of Stigmasterol and beta-Sitosterol on Nonalcoholic Fatty Liver Disease in a Mouse Model: A Lipidomic Analysis. J Agric Food Chem, 66(13): p. 3417-3425.
[22] Alkhalidy, H., W. Moore, Y. Wang, J. Luo, R.P. McMillan, W. Zhen, K. Zhou, and D. Liu, (2018) The Flavonoid Kaempferol Ameliorates Streptozotocin-Induced Diabetes by Suppressing Hepatic Glucose Production. Molecules, 23(9).
[23] Abdou, E.M., M.A.A. Fayed, D. Helal, and K.A. Ahmed, (2019) Assessment of the hepatoprotective effect of developed lipid-polymer hybrid nanoparticles (LPHNPs) encapsulating naturally extracted beta-Sitosterol against

CCl(4) induced hepatotoxicity in rats. Sci Rep, 9(1): p. 19779.
[24] Yuan, C., X. Zhang, X. Long, J. Jin, and R. Jin, (2019) Effect of beta-sitosterol self-microemulsion and beta-sitosterol ester with linoleic acid on lipid-lowering in hyperlipidemic mice. Lipids Health Dis, 18(1): p. 157.